SIMULATION OF MACHINE BACKGROUNDS

V. Talanov*
Institute for High Energy Physics, Protvino, Russia and TS/LEA Group, CERN

Abstract

The results of the numerical simulations of the machine background in the low luminosity experimental insertion regions IR2 and IR8 of the LHC are reviewed. The background sources considered include the beam-gas losses in the long straight sections, elastic scattering in the LHC cold sectors and the halo losses at the tertiary collimators. The scheme of the background shielding is also presented and the shielding efficiency for the collimation background is estimated as well.

INTRODUCTION

One of the possible definitions of the machine background describes it as the products of the secondary cascades, initiated by proton losses upstream and downstream of the beam interaction points (IPs), that reach the zones of the experiments from the machine tunnel [1]. Concerning the LHC Project, the first comprehensive review of this subject was done in the Workshop on LHC Backgrounds at CERN in 1996 [2]. There was introduced a concept of the background "scoring plane" (see Fig. 1) as a fictitious boundary between the machine and the experiment, where the simulated background tracks are recorded for the further analysis in the experimental detectors. Splitting the background calculations into two stages appeared to be absolutely critical for the background analysis, taking into account the unprecedented complexity of the Monte-Carlo calculations in both LHC and LHC experiments.

One of the purposes of the present review is an attempt to demonstrate a dramatic progress, achieved in understanding of this phenomenon during the past decade.

Because the machine background depends on the rate of the proton losses, this component of the secondary radiation in the experimental zones becomes visible with the very first bunch of the particles in the machine. Due to the same reason, the background rate scales with the intensity of the beam and not with the luminosity at the particular interaction point (apart from the component that is deter-

* Vadim.Talanov@ihep.ru, Vadim.Talanov@cern.ch

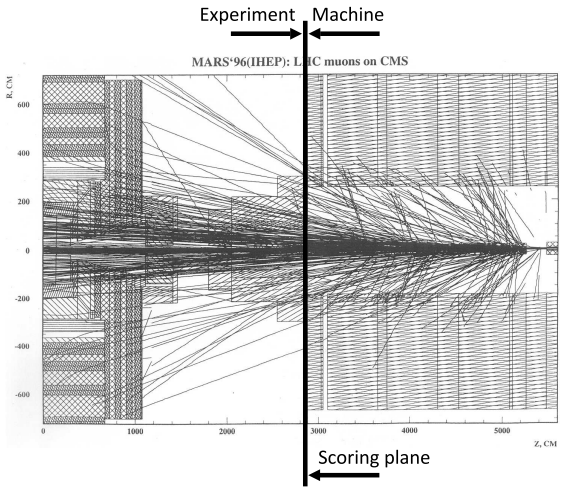

Figure 1: An illustration to the concept of the background "scoring plane" for the background analysis at the boundary between machine and experiment.

Figure 2: Installation of a part of the the ATLAS shielding in the UX15 cavern (a photo from the CERN Multimedia and Outreach Collection).

Figure 3: The frame of the blockhouse for the CMS forward shielding at the IHEP workshop (a photo from the IHEP Photo Gallery).

mined by the collision rate in the neighboring IPs). In detail, the background formation depends on practically every machine parameter — optics, apertures, filling scheme, residual gas density in the vacuum chamber, cleaning efficiency etc. — and their combination.

One of the passive measures to protect the experiments from the machine background is the installation of the background shielding at the entrance of the machine tunnel into the experimental zone. Due to the high luminosity in the IPs the LHC experiments at IP1 and IP5 were protected by such shielding from the machine background "by default" (see Fig. 2 and 3) while the shielding at IP2 and IP8 was missing and its configuration was proposed as a result of the presented background analysis.

BACKGROUND SOURCES

For a particular interaction point, the sources and origins of the machine induced background can be grouped as following (see Fig. 4):

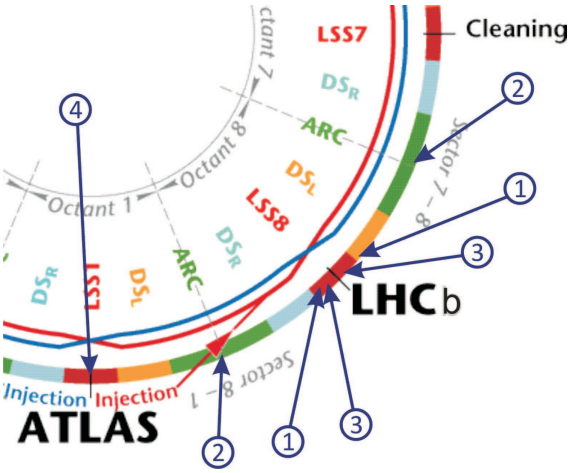

Figure 4: A part of the LHC scheme with the LHCb experiment at IP8 between the betatron cleaning insertion at IP7 and the ATLAS experiment at IP1 (the labels are explained in the text).

1. Beam-gas interactions in the Long Straight Sections (LSSs) that define a background component that strongly depends on the residual gas composition and density, and on the configuration of the limiting apertures in the LSS. An important feature is that the resulting products have a direct line of sight into the IP.

2. Elastic scattering of the beam particles on the residual gas in the cold sectors of the machine, which, depending on the scattering angle, may result in a proton loss at the next aperture limitation and thus strongly depends on the optics in the LSS.

3. Tertiary halo (also called "tails from collimation") that is comprised of the out-scattered protons not absorbed in the cleaning insertions and hence depends on the configuration of the collimation for a particular scenario of the machine operation. What is important is that the formation of the tertiary halo is different for LHC Beams 1 and 2 and for each IP a clear asymmetry of the tertiary losses is predicted.

4. Collisions in the neighboring IPs that can give a product lost in the next LSS upstream or downstream. This is the only background source that directly depends on the luminosity at some IP and so most probably can be considered relevant only for the case of the IP1 influence on the background at IP2 and IP8.

These background sources are evaluated below for the insertion regions IR2 and IR8, basing on the best available background estimates.

BEAM-GAS LOSSES IN THE LSSS

Simulation of the secondary cascades in the model of the LSS assuming the uniform distribution of the residual gas pressure gives the profile of the particle flux at the scoring plane depending on the layout of the insertion (see Fig. 5). As it was found, the dependence of the background flux from the beam-gas losses in the LSS on the machine optics was rather weak in the studied range of the β^* values at IP8 [3]. The absolute values for the background flux are obtained by the introduction of the residual gas density profile [4] for some period of the machine operation (see Fig. 6). The resulting distributions allow to study the formation of the background on the length of the LSS and to identify the background origins, as shown in Fig. 7.

In the nominal machine operation, the average H_2 equivalent density of 6.5×10^{12} mol/m^3 in the LSS results in the background muon flux of $\sim 10^6$ particles/s at the entrance to the IP2 experimental zone [5]. Apart from the fact that at the machine start-up period the predicted residual gas density can be factor 20 higher [4], one of the reasons to care

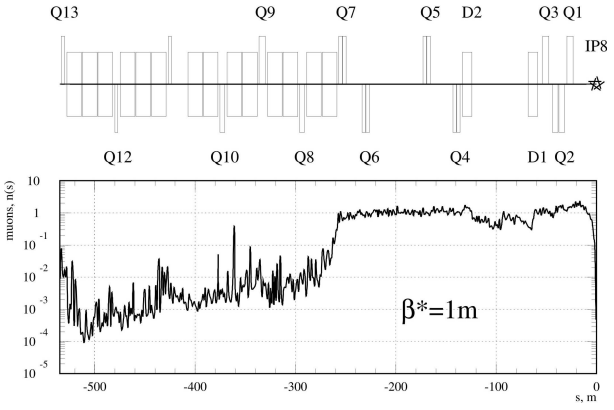

Figure 5: Number of the background muons at the IP7 side of IP8 as a function of the primary loss distance to the interaction point, given per unit of the linear density of the beam-gas loss rate in LSS8.

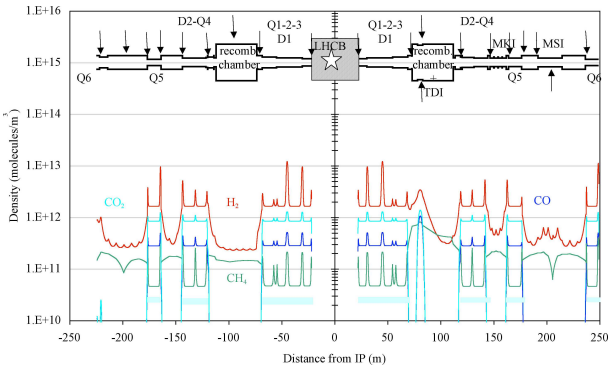

Figure 6: Density profiles for the different components of the residual gas in LSS8 (courtesy of A.Rossi).

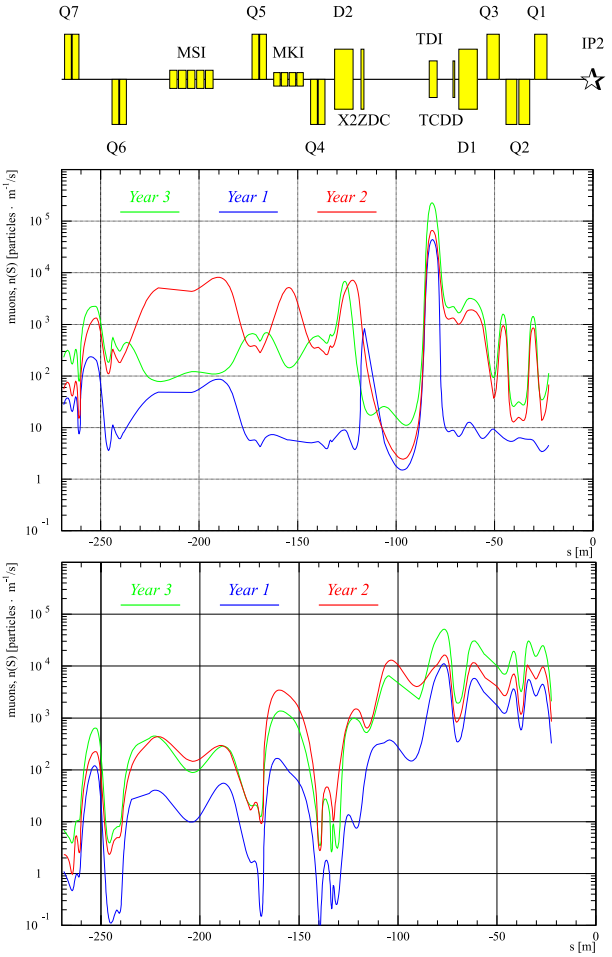

Figure 7: Number of the background muons as a function of the primary (top) and last (bottom) hadron-nucleus interaction distance to IP2, for three different scenarios of the machine operation.

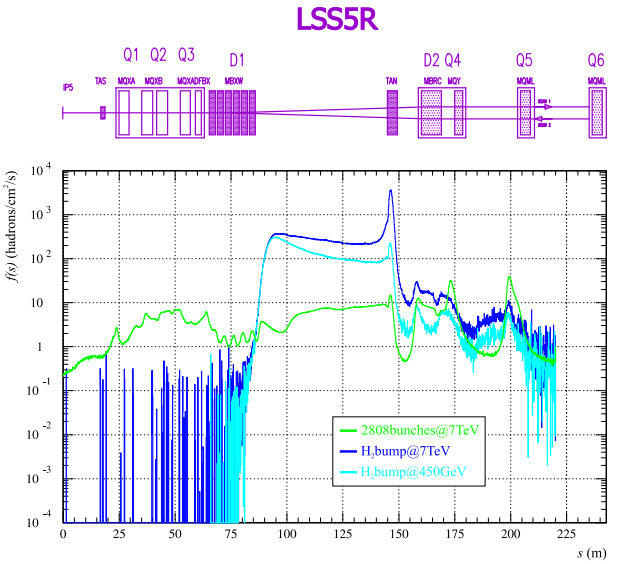

Figure 8: Hadron flux density $f(s)$ as a function of the distance to IP5, for three cases of the beam-gas losses in LSS5R considered.

about the beam-gas losses in the LSSs was studied in [6], considering the possible use of the radiation monitors as a vacuum diagnostic. It was taken as an input that a pressure bump 10. . .100 higher than the average gas density can exist locally for more than 100 hours due to the high NEG pumping capacity. The results of the calculations showed that in this case a few meter bump can produce the rate of the background compared to the whole LSS (see Fig. 8) and this increase in the background will most probably be the only way to detect the abnormal gas pressure.

SCATTERING IN THE COLD ARCS

Depending on the resulting angle the elastic scattering on the residual gas components may contribute to the primary beam halo, giving a proton that will be lost at the next aperture limitation, even before reaching the cleaning insertion. In the experimental insertion IR8, the losses in the low-β region between D1 dipole and Q1 quadrupole were found to be the most critical [7] (see Fig. 9). The sum of the background rates from the beam-gas losses in LSS8 and from the elastic scattering in the cold arcs, estimated using a very approximative value of 5×10^{14} mol/m^3 for H_2 equivalent gas density in the cryogenic vacuum chamber, is given in Table 1 for IR8, for several background components and different operation scenarios. As can be seen, the background rates at IP8 may vary from few MHz to few dozens of MHz, depending on the LHC Ring number and assumed vacuum conditions.

These estimates have been obtained without tertiary collimators (TCTs) that are by design a new aperture limitation in the LSSs. An attempt to evaluate the effect of the TCTs on the protons elastically scattered in the LHC cold sectors has been already done for the TCTs in IR1 at the

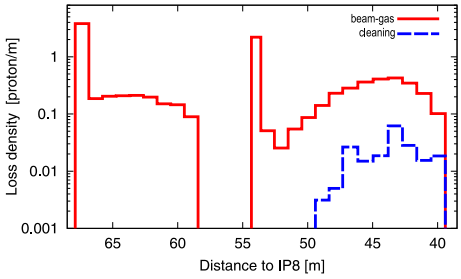

Figure 9: Loss density near the D1–Q1 low-beta section of LSS8L, for the beam-gas scattering in the section 78 (solid histogram) and the betatron cleaning inefficiency (dashed) (courtesy of I.Bayshev).

Type of particle	Particles per bunch (a) β^* = 1 m, I = 0.3 I_{n}			(b) β^* = 10 m, I = I_{n}		
	Ring 1 at -1 m from IP8			Ring 2 at 19.9 m from IP8		
	Year 2 Beginning (a)	Year 2 +10 days (a)	Year 3 +90 days (b)	Year 2 Beginning (a)	Year 2 +10 days (a)	Year 3 +90 days (b)
muons	1.07	0.015	0.008	1.42	0.026	0.030
neutrons	3.43	0.065	0.059	5.09	0.185	0.423
p + π + K	7.68	0.133	0.104	8.54	0.194	0.304
Total	12.18	0.213	0.171	15.05	0.405	0.756

Table 1: Rates of the background components at the IP8, [particles/bunch] for the LHC Ring 1 and 2, two options of β^* in the IR8 and three cases of the residual gas pressure at different stages of the machine operation.

13.5 σ distance from the beam [8]. It was found that up to 90 % of the halo protons that were previously lost on the apertures in IR1 are now intercepted by the TCTs, but the resulting flux of the background muons at the cavern entrance in this case is $\sim$ 4 times higher than from the beam-gas losses in the LSS itself (see Fig. 10).

BACKGROUND SHIELDING

Heavy shielding that protects the experiments at IP1 and IP5 from the secondary radiation from the collimator in front of the Q1 quadrupole also suppresses the machine background at the tunnel entrance into the experimental zones. Due to the low luminosity, initially there was no

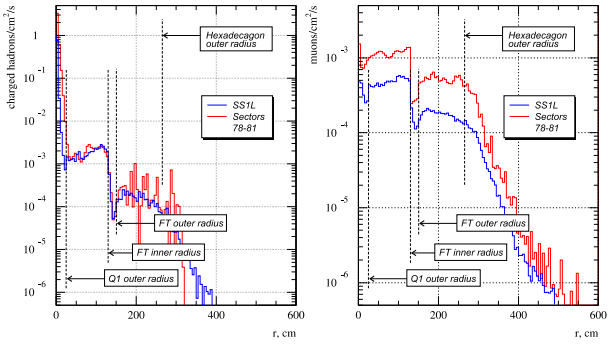

Figure 10: Charged hadron and muon flux density [particles/cm^2/s] at the UX15 entrance due to the beam-gas losses in LSS1L (blue) and sectors 78-81 (red).

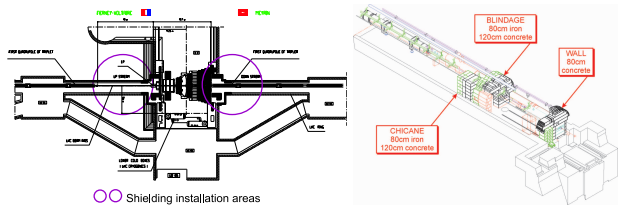

Figure 11: Top view of the UX85 cavern with the layout of the machine elements and the proposed locations of the background shielding (left) and layout of the shielding at the IR7 side of IR8 (right).

Figure 12: Machine background shielding in IR8, as installed at the IR1 side around the Q1 quadrupole (courtesy of D.Lacarrère).

such shielding at IP2 and IP8 until its position and configuration was proposed (see Fig. 11) basing on the background calculations and various mechanical constraints [9].

Full configuration of the shielding on both sides of IR8 includes 120 cm of concrete and 80 cm of iron, divided into blindage and chicane (an additional 80 cm concrete wall is installed at the IR7 side). Already installed (see Fig. 12) in IR8 "staged" configuration of the shielding has the reduced number of iron blocks. The effect of the shielding has been estimated for the background from the beam-gas losses in LSS8 and it was found that the full shielding reduces the charged hadron flux by a factor of 1.6–1.9 (and by a factor of $\sim$ 50 above the radius of 25 cm) and muon flux by a factor of 2.4–2.6, for the IR1 and IR7 sides of LSS8.

COLLIMATION BACKGROUND

Machine background from the tertiary losses in the LSS has been estimated for the case of the losses at two tertiary collimators installed in LSS8L (see Fig. 13). The distribution of the losses along the LHC Beam 1 has been calculated by the Collimation Project (see Fig. 14) for the full collimation and ideal machine, nominal settings of all collimators (TCTs in the IR8 at 8.3σ), nominal beam parameters and optics with the β^* of 10 m at IP8.

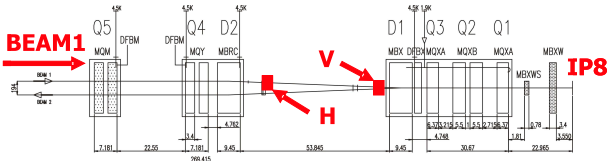

Figure 13: Positions of vertical and horizontal TCT collimator in LSS8L.

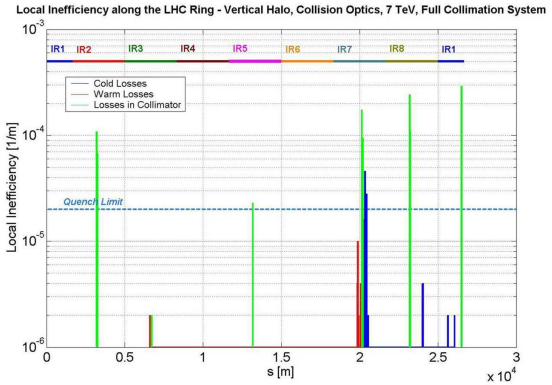

Figure 14: Loss distribution around the LHC Ring 1 for the primary losses at the betatron cleaning in IR7.

The cleaning inefficiency for the TCT(V,H) at the IR7 side of IR8 was estimated equal to $(0.84, 0.22)\times10^{-3}$ for the vertical halo and $(0.003, 0.3)\times10^{-3}$ for the horizontal one. To get the absolute values of the background particle fluxes, the value of 2.8×10^{9} protons/s for the losses on the primary collimators in IR7 was used that corresponds to the 30 h beam lifetime [10]. Under these conditions, the background from the losses at the TCTV is dominating, resulting in the flux of 5.7×10^{6} charged hadrons/s and 1.8×10^{6} muons/s at 1 m from the IP8 at the IR7 side [11]. These numbers are of the same order as the estimates for the background flux from both types of the beam-gas losses. The radial distribution of the collimation background is absolutely different — the particles from the beam-gas losses are the main contribution to the background around the beam line, while the collimation background clearly dominates at the large radii (see Fig. 15).

The efficiency of the staged shielding configuration was evaluated also for the collimation background in LSS8. Figure 16 gives the transverse distributions of the background flux within the tunnel entrance at the IR7 side of IP8, for the vertical halo losses at the TCTV. The full shielding at the IR7 side removes completely the charged hadron background and $\sim$ 2/3 of the background muons [11]. The efficiency of the staged shielding is less: $\sim$ 14 % of the charged hadrons and 45 % of muons are still visible after the shielding, mainly distributed in the areas where the iron shield is not installed.

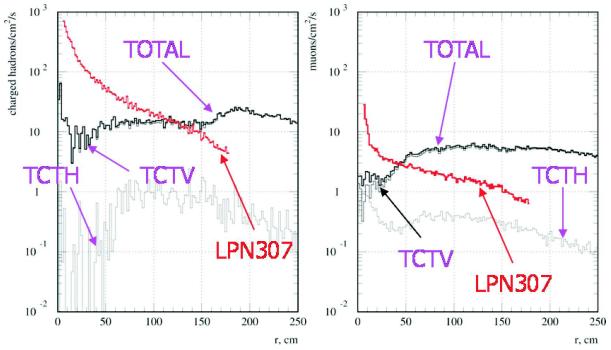

Figure 15: Particle flux density, [particles/cm^2/s] at 1 m from IP8, calculated for the losses at the TCTV/H, compared to the background from the beam-gas losses in LSS8L.

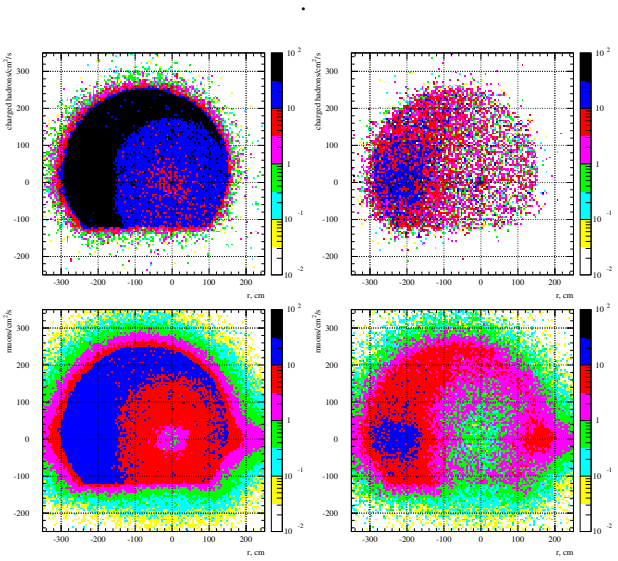

Figure 16: Particle flux density for charged hadrons (top) and muons (bottom), without (left) and with staged shielding (right).

BACKGROUND AT BRAN MONITORS

The issue of the machine background in IR2/8 is also extremely important for the operation of the collision rate monitors (BRANs) [12]. BRANs are installed in LSS2/8 in front of the D2 dipole, in the same region as the horizontal collimator TCTH. Contrary to the insertion regions IR1 and IR5, the detectors at this location are not shielded from the background from the tertiary collimator since there is no TAN absorber in the low luminosity insertions. In the case of the tertiary halo losses at the TCTH the BRANs in IR2/8 fall inside a peak of both charged and neutral background particle flux (see Fig. 17).

To estimate the background at the BRANs, the same set of the maps of the tertiary losses were used as in the evaluation of the background shielding in LSS8 (see Fig. 18). An example of the calculated background flux map at the BRAN is given in Fig. 19, compared to the distribution of

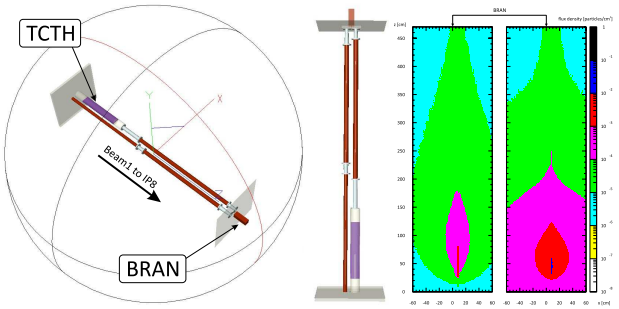

Figure 17: BRAN monitor position in the LSS8 (left) and the maps of charged and neutral components of the collimation background (right).

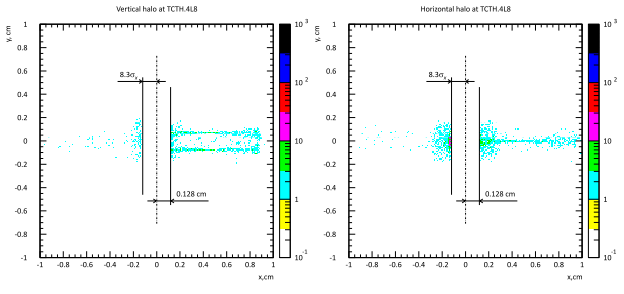

Figure 18: Vertical (left) and horizontal (right) tertiary halo losses at the TCTH in IR8.

the particles from the p-p collisions at the IP [13]. As can be seen, for the neutron flux density the estimated values are of the order of magnitude and equal to few 10^{-2} particles per primary event. For few 10^6 protons/s lost at the TCTH and 16 MHz event rate at IP8 this gives $\sim$ 10:1 signal to background ratio at the BRAN, for the neutron flux at the nominal machine operation.

However, if the rate of the losses at the TCTH will increase due to some abnormal spike of the halo, this ratio may change to the opposite one. The same is true for the BRAN operation at IP2 where the collisions are foreseen at the luminosity much lower than at IP8. Examining the loss distributions in Fig. 18, it may be proposed to put the collimators in IR2/8 in a more "relaxed" position since opening the TCT jaws just twice comparing to the assumed

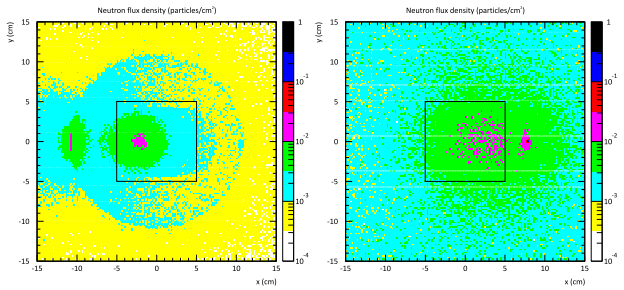

Figure 19: Neutron flux density per 1 p-p event in the IP (left) and per 1 proton lost at the TCTH (right).

settings would allow to decrease significantly the rate of the tertiary losses and the rates of the produced collimation background in the low luminosity insertions.

CONCLUSION AND OUTLOOK

Beam-gas losses in LSS2/8 and elastic scattering in the cold sectors of the machine between IP2/8 and the closest cleaning insertion in total result in the background flux at the entrance into the experimental zones of few 10^6 muons/s (hadron flux in a general case is an order of magnitude larger). For both sources of the beam-gas losses, a fresh set of the residual gas density estimates exist and the numbers above should be updated with these new estimates and the realistic model of the installed shielding in IR2/8.

Tertiary losses at the collimators in the experimental insertions, calculated for the nominal operation, add another few 10^6 muons/s to the background flux. The efficiency of the installed staged shielding for this background source is 86 % for charged hadrons and 55 % for muons, for the maximum of the tertiary losses at the IR7 side of IR8.

As it was shown, the rate of the collimation background (including the contribution from the primary halo losses at the TCTs due to the elastic beam-gas scattering) depends on the optimal settings of the collimators during nominal operation and start-up, and may be critical not only for the experiments at IP2 and IP8, but also for the luminosity measurement with the BRAN monitors.

ACKNOWLEDGMENTS

The author is grateful to K.M. Potter and E. Tsesmelis for the continuous support of this work in the TS/LEA Group.

REFERENCES

[1] G. Corti and V. Talanov, "Aspects of Machine Induced Background In The LHC Experiments", In: Proc. of the LHC Project Workshop — Chamonix XV, 2006, p.179–185.

[2] K.M. Potter (editor). Proc. of the Workshop on LHC Backgrounds, CERN, Geneva, March 22, 1996.

[3] I. Azhgirey, I. Baishev, K.M. Potter *et al.*, "Methodical Study of the Machine Induced Background Formation in the IR8 of LHC", LHC Project Note 258, CERN, Geneva, 2001.

[4] A. Rossi and N. Hilleret, "Residual Gas Density Estimations in the LHC Experimental Interaction Regions", LHC Project Report 674, CERN, Geneva, 2003.

[5] I. Azhgirey, I. Baishev, K.M. Potter *et al.*, "Machine Induced Background in the Low Luminosity Insertions of the LHC", LHC Project Report 567, CERN, Geneva, 2002.

[6] V. Baglin, V. Talanov, T. Wijnands, "Radiation monitors as a Vacuum Diagnostic for the Room Temperature Part of the LSS", LHC Project Note 378, CERN, Geneva, 2006.

[7] I. Baichev, J.B. Jeanneret, K.M. Potter, "Proton Losses Upstream of IP8 in LHC", LHC Project Report 500, CERN, Geneva, 2001.

[8] V. Talanov, "Estimation of the Machine Induced Background for the Commissioning Period with Tertiary Collimators in the IR1 of the LHC", LHC Project Note 371, CERN, Geneva, 2005.

[9] I. Azhgirey, I. Baishev, K.M. Potter *et al.*, "Evaluation of Some Options for Shielding from Machine Induced Background in the IR8", LHC Project Note 307, CERN, Geneva, 2002.

[10] R. Assmann, "Collimators and Cleaning: Could This Limit The LHC Performance ?", In: Proc. of the LHC Performance Workshop — Chamonix XII, 2003, p.163–170.

[11] R. Assmann, D. Macina, K.M. Potter *et al.*, "Tertiary Halo and Tertiary Background in the Low Luminosity Experimental Insertion IR8 of the LHC", In: Proc. of EPAC 2006, Edinburgh, p.532-534; LHC Project Report 953, CERN, Geneva, 2006.

[12] E. Bravin, S. Burger, C. Dutriat *et al.*, "Collision Rate Monitors for LHC", In: Proc. of PAC 2007, Albuquerque, p.4171-4173; LHC Project Report 1024, CERN, Geneva, 2007.

[13] H. Burkhardt, D. Macina, V. Talanov *et al.*, "Numerical Study of the Very Forward Background from the Proton-Proton Collisions in the Experimental Insertions of the LHC", In: Proc. of PAC 2007, Albuquerque, p.1619-1621; LHC Project Report 1049, CERN, Geneva, 2007.